Diagnosing the Influence of a Receding Snow Boundary on Simulated Midlatitude Cyclones Using Piecewise Potential Vorticity Inversion

MELISSA L. BREEDEN,[a] RYAN CLARE,[b] JONATHAN E. MARTIN,[c] AND ANKUR R. DESAI[c]

[a] *NOAA/OAR/ESRL/Chemical Sciences Laboratory, Boulder, Colorado*
[b] *Naval Research Laboratory, Monterey, California*
[c] *Department of Atmospheric and Oceanic Sciences, University of Wisconsin–Madison, Madison, Wisconsin*

(Manuscript received 20 February 2020, in final form 22 June 2020)

ABSTRACT: Previous research has found a relationship between the equatorward extent of snow cover and low-level baroclinicity, suggesting a link between the development and trajectory of midlatitude cyclones and the extent of preexisting snow cover. Midlatitude cyclones are more frequent 50–350 km south of the snow boundary, coincident with weak maxima in the environmental Eady growth rate. The snow line is projected to recede poleward with increasing greenhouse gas emissions, possibly affecting the development and track of midlatitude cyclones during Northern Hemisphere winter. Detailed examination of the physical implications of a modified snow boundary on the life cycle of individual storms has, to date, not been undertaken. This study investigates the impact of a receding snow boundary on two cyclogenesis events using Weather Research and Forecasting Model simulations initialized with observed and projected future changes to snow extent as a surface boundary condition. Potential vorticity diagnosis of the modified cyclone simulations isolates how changes in surface temperature, static stability, and relative vorticity arising from the altered boundary affect the developing cyclone. We find that the surface warm anomaly associated with snow removal lowered heights near the center of the two cyclones investigated, strengthening their cyclonic circulation. However, the direct effect of snow removal is mitigated by the stability response and an indirect relative vorticity response to snow removal. Because of these opposing effects, it is suggested that the immediate effect of receding snow cover on midlatitude cyclones is likely minimal and depends on the stage of the cyclone life cycle.

KEYWORDS: Cyclogenesis/cyclolysis; Extratropical cyclones; Potential vorticity; Regional models

1. Introduction

As the planet warms, the climatological southern edge of snow cover during boreal winter and spring is projected to move poleward (Manabe and Wetherald 1980; Brown 2000; Lemke et al. 2007; Gan et al. 2013). Rydzik and Desai (2014) found that there was a statistical relationship between the location of the snow boundary, low-level baroclinicity, and cyclone tracks, presumably related to enhanced radiative, thermal, and moisture gradients along the snow line. Consequently, it is possible that changes in the snow boundary could impact aspects of developing cyclones over the next century.

The large-scale, low-frequency circulation response to receding snow cover has been investigated previously and is nonnegligible. Ross and Walsh (1986) used the National Center for Atmospheric Research Community Forecast Model to force anomalous snow extent over North America, which, months later, induced remote temperature responses over Scandinavia and western Europe. Klingaman et al. (2008) examined the large-scale response to anomalous Great Plains snow cover imposed in simulations using the Community Atmosphere Model and found a response in Eurasian temperatures related to a positive North Atlantic Oscillation that developed at a lag of several months. Sobolowski et al. (2010) examined the low-frequency, large-scale atmospheric response to a persistent snow cover anomaly using a pair of 40-member atmospheric general circulation model simulations with high- and low-snow forcing, and also found a transient eddy response in the North Atlantic storm track due to anomalous snow cover over North America.

A separate question that has also received research attention is–what is the immediate (i.e., occurring within days following production of a snow cover anomaly), regional atmospheric response to snow cover? Using a one-dimensional snowpack model, Ellis and Leathers (1999) simulated the effect of snow removal on four cold air masses that developed in the Great Plains region of the United States. They found that for all four cases, the air masses warmed on average by 6°–10°C during the daytime, and by 1°–2°C during nighttime, primarily through sensible heat fluxes from the ground to the air mass. Elguindi et al. (2005) compared the intensity and sensible weather associated with cyclogenesis in the Great Plains of North America for cases with the observed snow boundary and for simulations with snow completely covering the model domain. They found that covering the domain with snow led to weaker mean sea level pressure minima, weaker fronts and thermal advection, and reduced precipitation and cloud cover due to weaker vertical motion. Perhaps directly related to the former pair of attributes, increased static stability of the lower troposphere was also characteristic of the snow-covered domain.

Previous research examining how a change in snow cover affects the development of extratropical cyclones has focused on the presence of more-than-typical snow cover and colder

Corresponding author: Melissa L. Breeden, melissa.breeden@noaa.gov

DOI: 10.1175/MWR-D-20-0056.1

than normal temperatures. Whether the tropospheric response and influence on cyclones in the *absence* of snow and *warmer* than normal temperatures produce an equal and opposite response remains to be determined. In the present study, we have designed modeling experiments to test if the removal of snow will affect the strength and/or trajectory of developing cyclones over North America. The removal of snow is hypothesized to increase low-level temperature and consequently reduce static stability. To isolate the direct and indirect effects snow removal has on the circulation, we applied piecewise quasigeostrophic potential vorticity (QGPV) inversion. The inversion technique can isolate the geopotential height response to changes in 1) surface temperature, 2) static stability, and 3) low-level relative vorticity, that arise due to the removal of snow. It is reasonable to anticipate that the warm surface temperature anomaly associated with snow removal, manifests itself as a cyclonic QGPV anomaly (Bretherton 1966), and as a result, enhances the circulation of amplifying cyclones. Additionally, we suppose that the vertical structure of the resultant surface warm anomaly will reduce the static stability of the environment near the cyclone, which can enhance vertical motion, cloud cover and precipitation.

The paper is organized as follows. Section 2 describes both the modeling simulations designed to test the immediate impact snow removal has on cyclogenesis as well as the potential vorticity inversion technique used for analysis. Section 3 presents results from two selected cases, including a synoptic overview and results from QGPV inversion. A discussion of results and concluding remarks are offered in section 4.

2. Method

To test the hypothesized influence of snow removal on cyclogenesis, a suite of model simulations was designed that uses the observed snow boundary position (the control simulation) and a range of plausible changes to the snow line as projected by climate models [see Clare (2018) for more details]. The difference in geopotential height between the control and modified simulations was calculated throughout the troposphere for each case. The resultant height anomaly fields were then used for piecewise potential vorticity inversion, to isolate and quantify the direct and indirect effects, such as changes in temperature and static stability, the modified snow boundary had on the circulation.

a. Simulation design

We ran simulations using the Weather Research and Forecasting Model, version 4.0.3, with 30-km grid spacing for 20 subjectively selected cyclone cases that occurred during boreal winter (November–March; Skamarock et al. 2019). The domain for this study includes the continental United States as well as much of Canada and Mexico and is centered over the Great Plains region. A grid cell was identified as snow covered if the simulated snow mass was at least 5 kg m^{-2}, corresponding to a snow depth of about 5 cm assuming a 10:1 snow-to-water ratio. Output from 14 models of phase 5 of the Coupled Model Intercomparison Project (CMIP5; Table 1), using the representative concentration pathway 4.5 and 8.5 scenarios, was used to determine a range of possible modifications to the position of the snow boundary by the year 2100 that could arise from future changes in greenhouse gas concentrations. Each of the CMIP5 models used to determine the ranges of snow boundary retreat applied in this experiment are present in the study of 22 CMIP5 models by Brutel-Vuilmet et al. (2013). They found that though the models did not adequately capture significant long-term snow mass reductions in spring, when ensemble-averaged, the models studied were able to realistically reproduce observed snow water equivalent in the period from 1979 to 2005. Eight of those models were ultimately excluded from consideration in this experiment as a result of restricted data availability, resolution issues, or large regional biases. The remaining model simulations were sorted based upon their projected changes to the snow boundary. For each simulation, the monthly mean change in the snow line between the 2080–99 and 1986–2005 periods was determined. The projected changes were then grouped into 10th-, 50th-, and 90th-percentile categories. For each of our selected cases, we ran simulations with each percentile's poleward snow line retreat (10th, 50th, and 90th) applied to the observed snow boundary, as well as a simulation with complete snow removal.

In addition, simulations for each case and percentile of snow line retreat were initialized at a range of 0–4 days prior to cyclogenesis at 24-h intervals, ultimately yielding 500 distinct simulations. Information regarding the overall results of all simulations can be found in Clare 2018). Here, two cyclogenesis cases were selected for in-depth analysis. We opt for the case study approach at first, to highlight the processes by which snow cover *can* affect cyclogenesis, before attempting to generalize results with composite analysis of all cases. Problems with a composite inversion can be numerous, particularly given the different relationship between each cyclone trajectory and the underlying snow cover, different large-scale conditions, and different regions of origin among the selected cases. We compare simulations of the two selected cases initialized 4 days prior to cyclogenesis, and consider differences between the control and 90th-percentile simulations, to analyze the strongest response to snow removal while remaining within the range of plausible future changes. Results summarizing the response in all 500 model simulations can be found in Clare (2018). Model output was interpolated to pressure surfaces at 50-hPa intervals from 1000 to 100 hPa at 6-hourly temporal resolution and was regridded onto a $1° \times 1°$ latitude–longitude grid.

b. Anomaly calculations

We use a potential vorticity inversion approach (described in section 2c) that employs geopotential height on pressure surfaces to calculate and invert QGPV. To keep our view of the cases consistent with the inversion framework, we consider the evolution of the surface cyclone on pressure surfaces as well. Using each case's control simulation, the mean state $\overline{z}$ was defined as the 7-day average over which each selected cyclone developed, corresponding to 0000 UTC 3 March 2005–1800 UTC 9 March 2005 and 0000 UTC 22 January 1996 and 1800 UTC 28 January 1996. To track the geopotential height minimum associated with each surface cyclone, we calculated geopotential height anomalies, $z' = z - \overline{z}$. The evolution of

TABLE 1. CMIP5 models used to determine the range of likely changes in the position of the snow/no snow boundary through the year 2100. Expansions of the model names can be found at https://www.ametsoc.org/PubsAcronymList.

Modeling center (or group)	Institute identifier	Model name	Horizontal resolution (°lon × °lat)	No. of vertical levels
Commonwealth Scientific and Industrial Research Organisation (CSIRO) and Bureau of Meteorology (BoM), Australia	CSIRO-BoM	ACCESS1.0	1.875 × 1.25	38
National Center for Atmospheric Research	NCAR	CCSM4	1.25 × 1.0	26
Centre National de Recherches Météorologique/Centre Européen de Recherche et Formation Avancée en Calcul Scientific	CNRM-CERFACS	CNRM-CM5	1.4 × 1.4	31
Commonwealth Scientific and Industrial Research Organisation in collaboration with Queensland Climate Change Centre of Excellence	CSIRO-QCCCE	CSIRO Mk3.6.0	1.8 × 1.8	18
NASA Goddard Institute for Space Studies	NASA GISS	GISS-E2-H; GISS-E2-R	2.5 × 2.0	40
Met Office Hadley Centre	MOHC	HadGEM2-CC; HadGEM2-ES	1.8 × 1.25	60
Russian Institute for Numerical Mathematics	INM	INM-CM4	2.0 × 1.5	21
Atmosphere and Ocean Research Institute (The University of Tokyo), National Institute for Environmental Studies, and Japan Agency for Marine-Earth Science and Technology	MIROC	MIROC5	1.4 × 1.4	40
Max Planck Institute for Meteorology	MPI-M	MPI-ESM-LR	1.9 × 1.9	47
Meteorological Research Institute	MRI	MRI-CGCM3	1.1 × 1.1	48
Norwegian Climate Centre	NCC	NorESM1-M; NorESM1-ME	2.5 × 1.9	26

the surface cyclone was then considered using the 1000-hPa z' fields in each case. To determine the change in the height and temperature fields arising from the imposed retreat of the snow boundary, the control simulation height fields were subtracted from those of the 90th-percentile snow-removal simulations: $z'' = z_{90} - z_{\mathrm{CTRL}}$. Temperature anomalies due to removal of snow were calculated in the same manner: $T'' = T_{90} - T_{\mathrm{CTRL}}$.

c. *Quasigeostrophic potential vorticity inversion*

We used piecewise QGPV inversion to test the hypothesized impact on the geopotential height field of the near-surface temperature anomaly created by removing snow. The QGPV approach is particularly amenable to the present analysis, as the components of QGPV linearly combine to produce the observed geopotential height field. QGPV is defined as the sum of the planetary vorticity, geostrophic relative vorticity, and a function of static stability:

$$q = f + \frac{1}{f_o}\nabla^2\phi + f_o\frac{\partial}{\partial p}\left(\frac{1}{\sigma}\frac{\partial\phi}{\partial p}\right), \tag{1}$$

where $\nabla^2 = (\partial^2/\partial x^2, \partial^2/\partial y^2)$ is the two-dimensional Laplacian, ϕ represents deviations from the reference atmosphere geopotential, f_o is the Coriolis parameter, and σ is the reference atmosphere static stability [$\sigma = -(\alpha/\theta)d\theta/dp$], where α is specific volume. To investigate the changes in QGPV associated with a receding snow line, we calculated QGPV anomalies using the z'' and T'' fields for each case, and split the anomalies into contributions from relative vorticity and static stability [Eqs. (2) and (4), below]. Horizontal variations in geopotential manifest themselves in the geostrophic relative vorticity term [Eq. (2)] so that in the Northern Hemisphere cyclones are characterized by relative vorticity maxima and positive QGPV anomalies and anticyclones are characterized by relative vorticity minima and negative QGPV anomalies:

$$q''_\zeta = \frac{1}{f_o}\nabla^2\phi''. \tag{2}$$

The vertical gradient of geopotential is related to temperature, T, through the hydrostatic relationship [Eq. (3)]. As a result, QGPV is also proportional the vertical change of temperature (and temperature anomalies) and therefore to atmospheric stability, with stability maxima corresponding to positive QGPV anomalies and vice versa [Eq. (4)]:

$$\frac{\partial\phi''}{\partial p} = -\frac{R}{p}T'' = -\frac{R}{p}\left(\frac{p}{p_o}\right)^{\kappa}\theta'' \quad \text{and} \tag{3}$$

$$q''_{\mathrm{st}} = f_o\frac{\partial}{\partial p}\left(\frac{1}{\sigma}\frac{\partial\phi''}{\partial p}\right). \tag{4}$$

As such, regions in which temperature decreases rapidly with height are characterized by reduced stability and QGPV minima. Anywhere temperature increases with height (or decreases less rapidly), is, conversely, associated with enhanced stability and QGPV maxima.

Bretherton (1966) showed that surface potential temperature θ anomalies could be considered to be QGPV anomalies, and in particular that surface warm and cold anomalies act as cyclonic and anticyclonic QGPV anomalies, respectively. We include the model-output T''/θ'' anomalies as a Neumann boundary condition at the lower boundary (1000 hPa) via

Eq. (3) and solve for the height field without any interior QGPV values, to determine the nonlocal response to the 1000-hPa temperature anomalies produced by snow removal. The resultant geopotential anomaly shall be referred to as ϕ''_θ and represents the balanced, troposphere-deep height response to the surface θ'' anomaly. To check whether the temperature changes near the surface are well captured by the 1000-hPa temperature or height values, we compared the surface and 1000-hPa output temperature anomalies, and we found that, while there was a minor reduction in the 1000-hPa temperature anomaly relative to the surface, the structure and magnitude overall agreed reasonably well.

Holopainen and Kaurola (1991) demonstrated that one can partition QGPV anomalies in various ways, including inversion of the relative vorticity, stability and surface temperature components separately or inversion of anomalies within different vertical layers. For our purposes of isolating the surface temperature impact on the circulation, we calculated the QGPV anomalies associated with surface temperature anomalies, relative vorticity and stability separately. We then determined the nonlocal impact each of these QGPV anomalies has on the circulation by inverting each anomaly separately, to retrieve its associated geopotential height fields [Eq. (5)]. Inversion was performed using an iterative successive over-relaxation technique:

$$z'' = z''_\theta + z''_\zeta + z''_{\rm st} = \frac{1}{g}[\phi''_\theta + \mathcal{L}^{-1}(q''_\zeta) + \mathcal{L}^{-1}(q''_{\rm st})]. \qquad (5)$$

In this manner, we were able to test our hypothesis regarding the suspected impact of removing snow on the height field near developing cyclones in the two cases examined. There is substantial cancellation between the surface temperature and stability response (which we explore in section 3), so for brevity we consider these terms as a net temperature/stability height anomaly, $z''_T = z''_\theta + z''_{\rm st}$, in some of the following analysis.

3. Results

Two cases were selected for investigation in this study, based upon their differences in time of year, origin, and trajectory with respect to the snow boundary. The first case examined was a typical Alberta Clipper that developed in northwesterly flow in early March 2005, crossing from north to south of the snow line during its evolution. The second was a lee-cyclogenesis case that developed east of the Rockies and propagated to the northeast thereafter, crossing from south to north of the snow boundary. The immediate effect of snow removal (i.e., occurring within 1 week following removal) in the two cases is shown in Fig. 1.

Regions of warm 1000-hPa temperature anomalies are observed in both cases and are broadly collocated with the area over which snow was removed. For the March 2005 case, the snow line ran from northwest to southeast over the continental United States, a shape that is imitated in the 90th-percentile removal simulation snow line located farther north (Fig. 1a). The 1000-hPa warm anomalies developed over the removal of snow and were strongest over the upper Midwest and southern

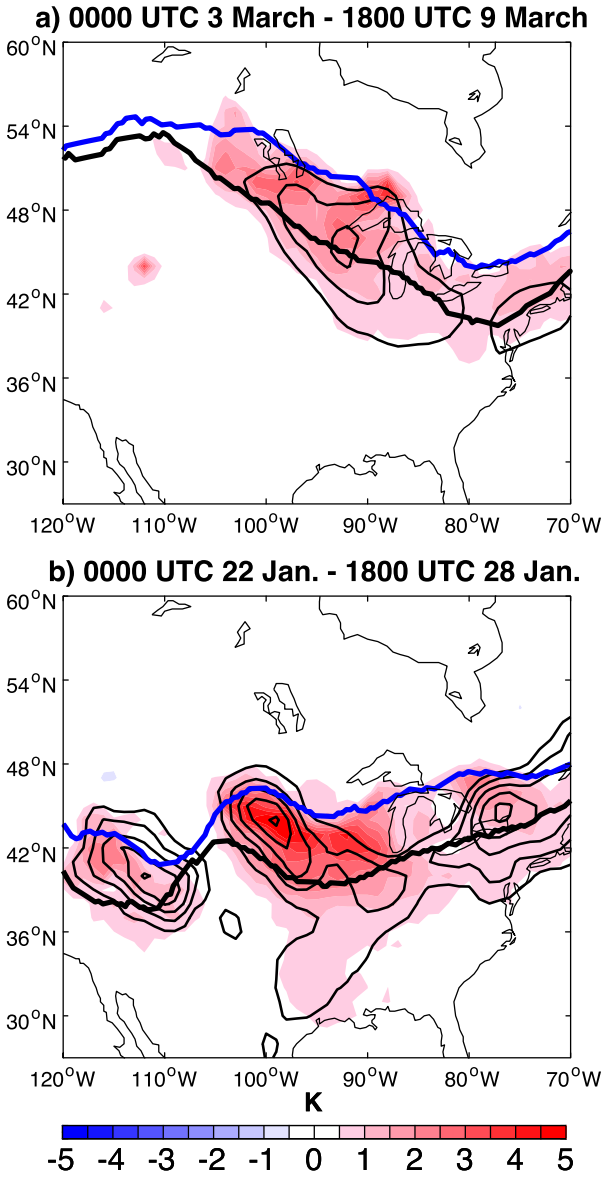

FIG. 1. Location of snow boundary in control (thick black line), along with 90% removal simulations (thick blue line), including simulated 7-day-average 1000-hPa temperature anomaly (color shading) and 7-day-average 1000-hPa height anomalies, negative values only, beginning at −2 m contoured every 1 m (thin black lines), for (a) 0000 UTC 3 Mar–1800 UTC 9 Mar 2005 and (b) 0000 UTC 22 Jan–1800 UTC 28 Jan 1996.

Canada. The anomalies extend farther south than the area of snow removal, presumably a result of mixing and advection of these anomalies by the circulation.

The January 1996 case exhibited a snow boundary that cut more directly west–east across the continent, and in this case the temperature anomalies were characterized by three local maxima over Nevada, the Great Plains, and southern Ontario (Fig. 1b). In both cases weak negative height anomalies accompanied the warm temperature anomalies at 1000 hPa,

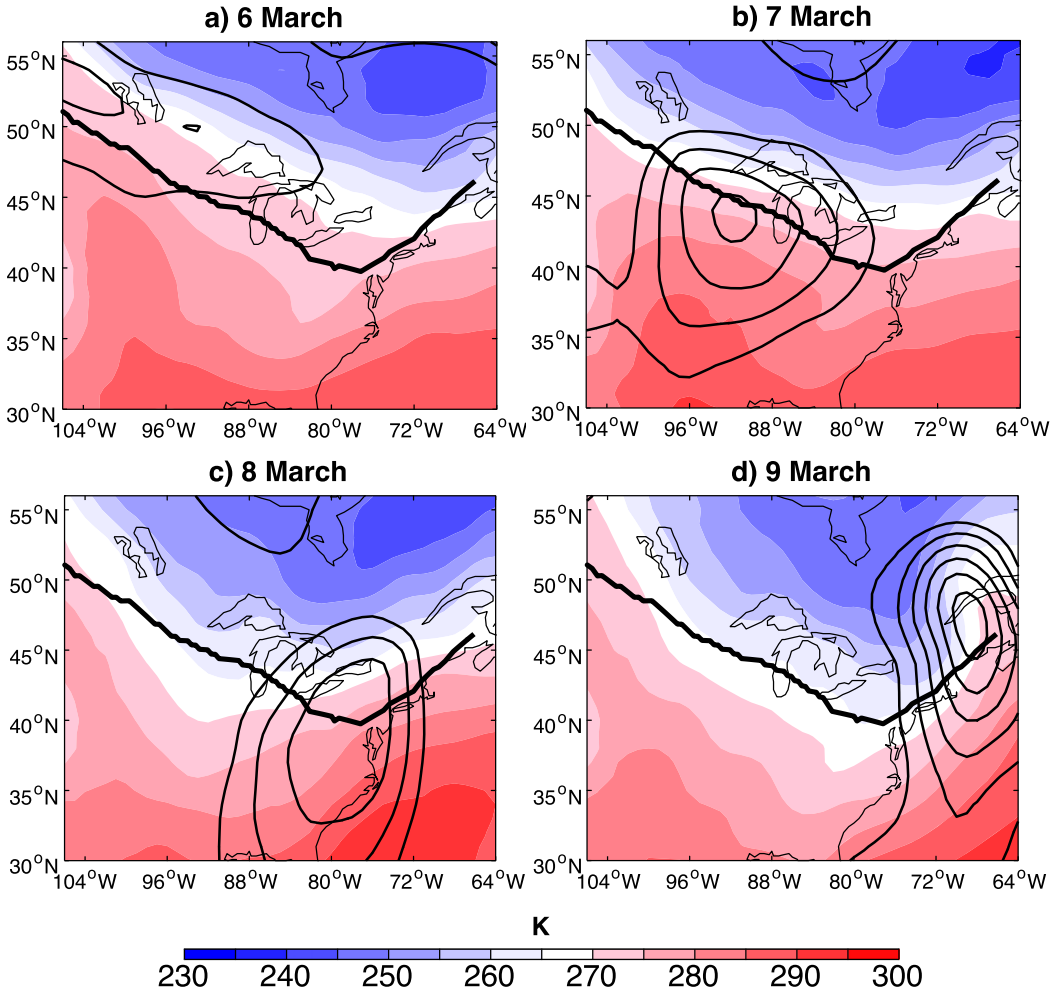

FIG. 2. The daily mean 1000-hPa temperature (color shading) and 1000-hPa z' field (anomalies calculated with respect to the 0000 UTC 3 Mar–1800 UTC 9 Mar average; thin black contours, contoured every 25 m starting at −25 m), negative values only, for (a) 6, (b) 7, (c) 8, and (d) 9 Mar 2005. Fields are shown for the control simulation. The thick black line marks the location of the snow line in the control simulation.

consistent with the notion that a surface warm anomaly produces a cyclonic QGPV/height anomaly.

a. March 2005 case

The cyclone in this case began as a depression aligned along a region of strong baroclinicity on 6 March that subsequently slid southeastward and amplified one day later over Wisconsin (Figs. 2a,b). By that time the region of strongest baroclinicity was located just north of the snow line, and the cyclone tracked roughly along the snow line as it propagated and amplified. The cyclone weakened slightly on 8 March (Fig. 2c), subsequently deepening rapidly (likely aided by ingestion of warm, moist air from over the Atlantic Ocean) as it propagated to the northeast on 9 March (Fig. 2d). By this time the cyclone also exhibited a well-developed thermal structure including a prominent cold front.

In the 90th-percentile simulation, negative z'' anomalies developed near the surface just to the east of where the cyclone began to develop on 6 March, over the region of snow removal and farther to the south as well (Fig. 3a). The negative height anomalies strengthened thereafter, overlapping with the cyclone center (and therefore deepening the height minimum of the cyclone) on 7 and 8 March (Figs. 3b,c). Regions of positive height anomalies developed on 8 March, near the modified snow boundary, strengthening on 9 March in the cyclone's northwest quadrant (Fig. 3d). Supporting our initial hypothesis, positive temperature anomalies were roughly collocated with the negative height anomalies on 6–7 March (Fig. 4). Later in the cyclone life cycle, however, the direct relationship between the temperature and height anomalies weakens. By 8 March, and increasingly by 9 March, the correspondence between the temperature and height anomalies is rather poor, with the warm anomalies remaining in the area of snow removal, while positive height anomalies developed over much of eastern Canada over the snow-covered region and negative height anomalies formed south

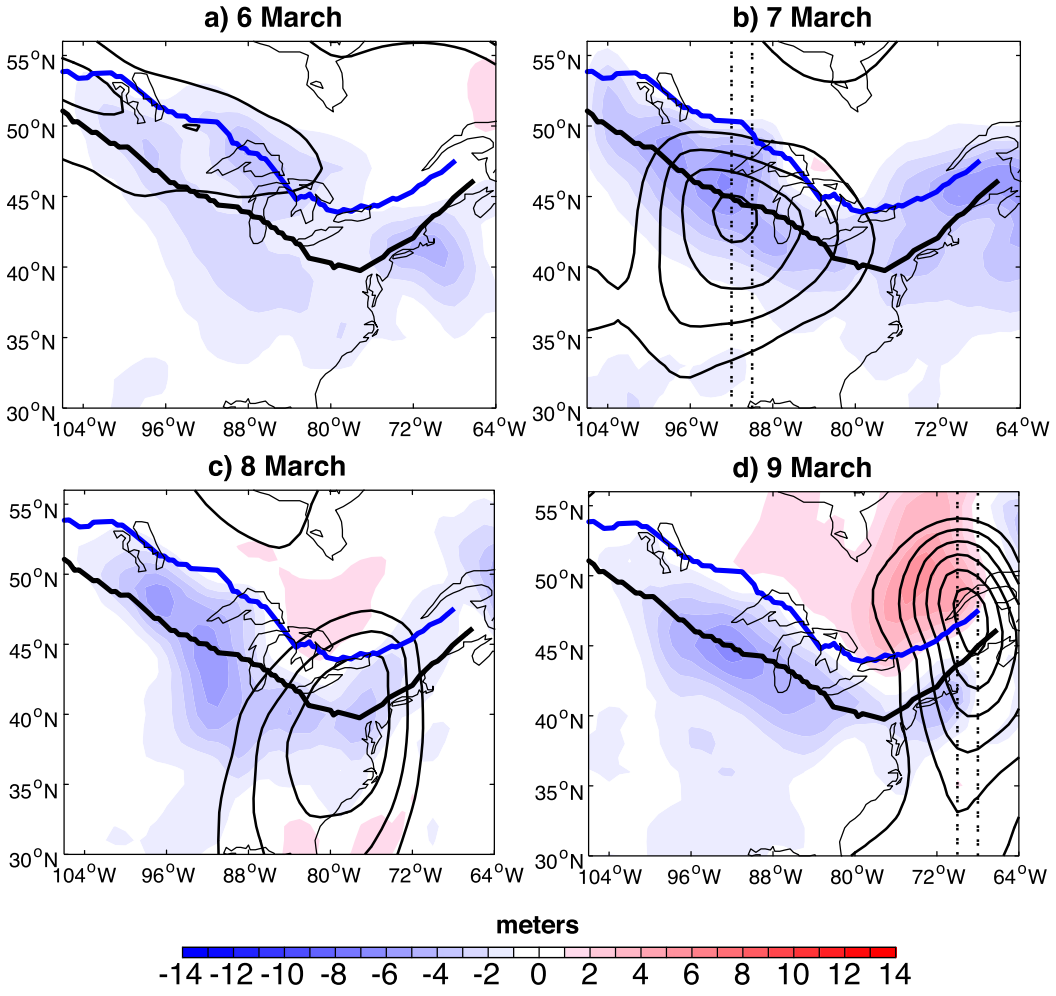

FIG. 3. The daily mean 1000-hPa z'' field (anomalies calculated as the difference: 90th-percentile simulation − control simulation; color shading) at (a) 6, (b) 7, (c) 8, and (d) 9 Mar 2005. The thin black contours show the 1000-hPa z' field, calculated with respect to the 0000 UTC 3 Mar–1800 UTC 9 Mar average, contoured every 25 m starting at −25 m, negative values only. The thick black line marks the location of the snow line in the control simulation, and the thick blue line shows the snow line in the 90th-percentile snow-removal simulation. The dashed lines in (b) and (d) mark the location of cross sections presented in Fig. 5, below.

of the snow boundary in the midwestern United States (cf. Fig. 3d, Fig. 4d).

Cross sections of height and temperature anomalies (z'' and T''), taken at the times and locations marked in Figs. 4b and 4d, indicate that on 7 March the 1000-hPa negative height anomaly observed over the cyclone center extends only to 800 hPa, at which point the sign of the height anomalies reversed to positive north of 45°N (Fig. 5a). The surface warm anomaly is similarly shallow, with a very weak temperature response in the mid- and upper troposphere (Fig. 5c). Two days later on 9 March, the negative height anomaly at the surface has weakened substantially, while a stronger positive height anomaly has developed through much of the troposphere, at some points extending all the way to the surface, such as at 50°N (Fig. 5b). The surface warm anomaly observed on 7 March has weakened in magnitude as well and now extends to about 500 hPa, tilting slightly northward with increasing altitude (Fig. 5d). A negative temperature anomaly located from 200 to 300 hPa developed by this time, located just above the maximum in the positive height anomaly.

It therefore appears that early in the cyclone life cycle the removal of snow enhanced the cyclonic circulation near the surface. Later, this effect weakened as it was negated by a broad increase in heights above the surface. Upper-tropospheric cooling is observed from 200 to 300 hPa [consistent with presence of the height anomalies that are decreasing with height; Eq. (3)] revealing that, although weak, changing the lower boundary had an impact all the way to the tropopause. The structure of the height response to snow removal on 7 March resembles the Saharan heat low, a warm-core low pressure center that is strongest near the surface and transitions to an upper-level anticyclone near 700 hPa (Lavaysse et al. 2009). Heat lows are surface-driven, which may explain why their structure resembles the height response to snow removal.

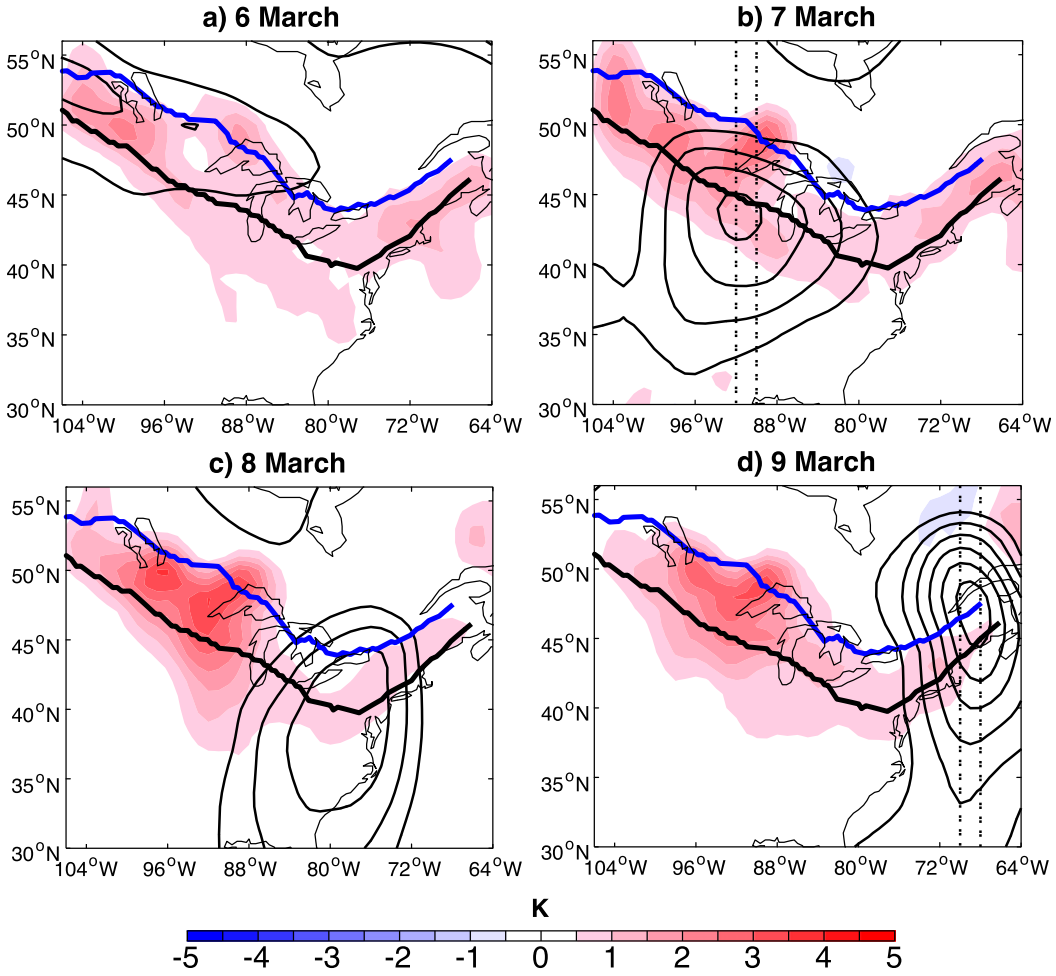

FIG. 4. As in Fig. 3, but with the color shading showing the daily mean difference in 1000-hPa t'' field.

The anticyclonic anomaly subsequently strengthened over time as observed on 9 March, at some locations extending to the surface.

Cross sections of the height fields attained from inverting the combined temperature term ($z''_T = z''_\theta + z''_{\rm st}$) and relative vorticity components of the QGPV indicate that, as suspected, the temperature term is responsible for the majority of the strong, shallow height anomaly observed on 7 March (Figs. 6a,b). Above 800 hPa, the temperature and vorticity components both contribute to positive height anomalies north of 45°N while the vorticity component produced negative anomalies to the south (Fig. 6c). Overall, the patterns of the height responses from z''_T and z''_ζ are notably different, with the temperature contribution displaying strong variations with height, meaning it is overall baroclinic, while the relative vorticity contribution is more constant with height and thus overall barotropic. Further partitioning the temperature term into contributions from static stability and the surface temperature anomaly illustrates the strong cancellation between these two terms (Fig. 7). The warm 1000-hPa temperature anomaly is treated as a positive QGPV anomaly, inducing a cyclonic height anomaly as anticipated (Fig. 7a). The vertical structure of a positive temperature anomaly that decreases with height increases the environmental lapse rate, reducing the stability and therefore producing a negative QGPV anomaly. Correspondingly, inversion of $q''_{\rm st}$ produces an anticyclonic height anomaly (Fig. 7b). The sum of these two opposing aspects related to temperature and stability indicates that, at this time and location, the cyclonic effect of the surface temperature anomaly is just slightly stronger than the anticyclonic anomalies produced by the stability term, leading to a net negative anomaly at the surface (Fig. 7c). Above 700 hPa, the stability influence is stronger and positive height anomalies result (Fig. 7c and Fig. 6b, which both show z''_T but at different contour intervals). Similar cancellation was observed by Holopainen and Kaurola (1991) using a prescribed surface temperature and vertical temperature distribution, although the cancellation occurred higher in the troposphere near 500 hPa.

Two days later on 9 March, the cyclonic 1000-hPa height anomaly over the cyclone center weakened, due to a weaker negative anomaly associated with the z''_T term (Figs. 8a,b). Simultaneously, the z''_ζ term contributed more strongly to the height field, producing positive height anomalies throughout

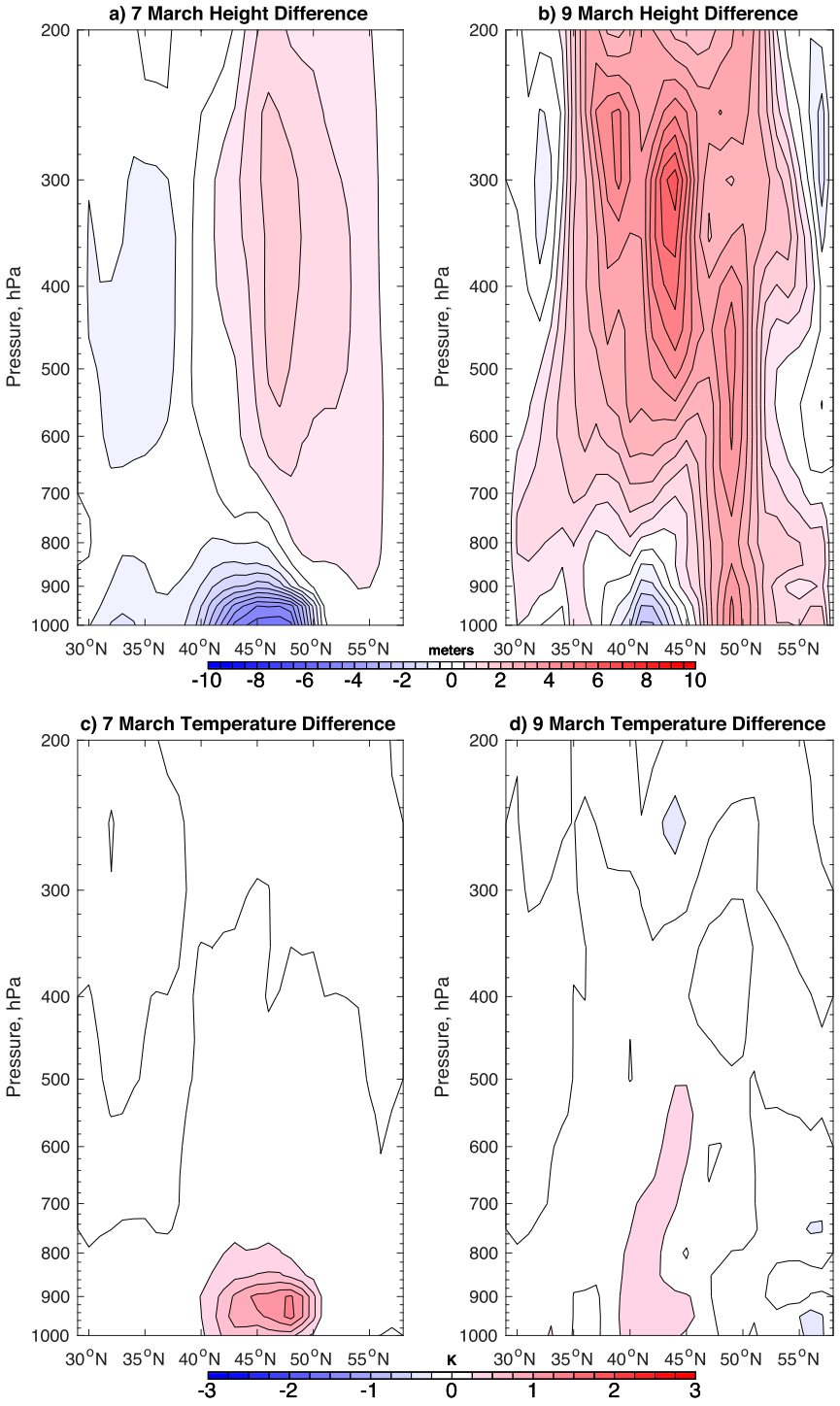

FIG. 5. Cross sections of (a),(b) z'' and (c),(d) t'' taken at the locations and times shown in Figs. 4b and 4d: (left) 7 Mar averaged from 268° to 270°E and (right) 9 Mar averaged from 290° to 292°E.

most of the troposphere, with maxima from 300 to 400 hPa from 35° to 45°N and from 800 to 1000 hPa at 50°N (Fig. 8c). Overall the height response appears more dominated by the relative vorticity contribution to development, in contrast to the 7 March cross section in which the surface temperature effect was strongest.

The influence of the surface warm anomaly produced by removing snow therefore appears to incite a direct effect

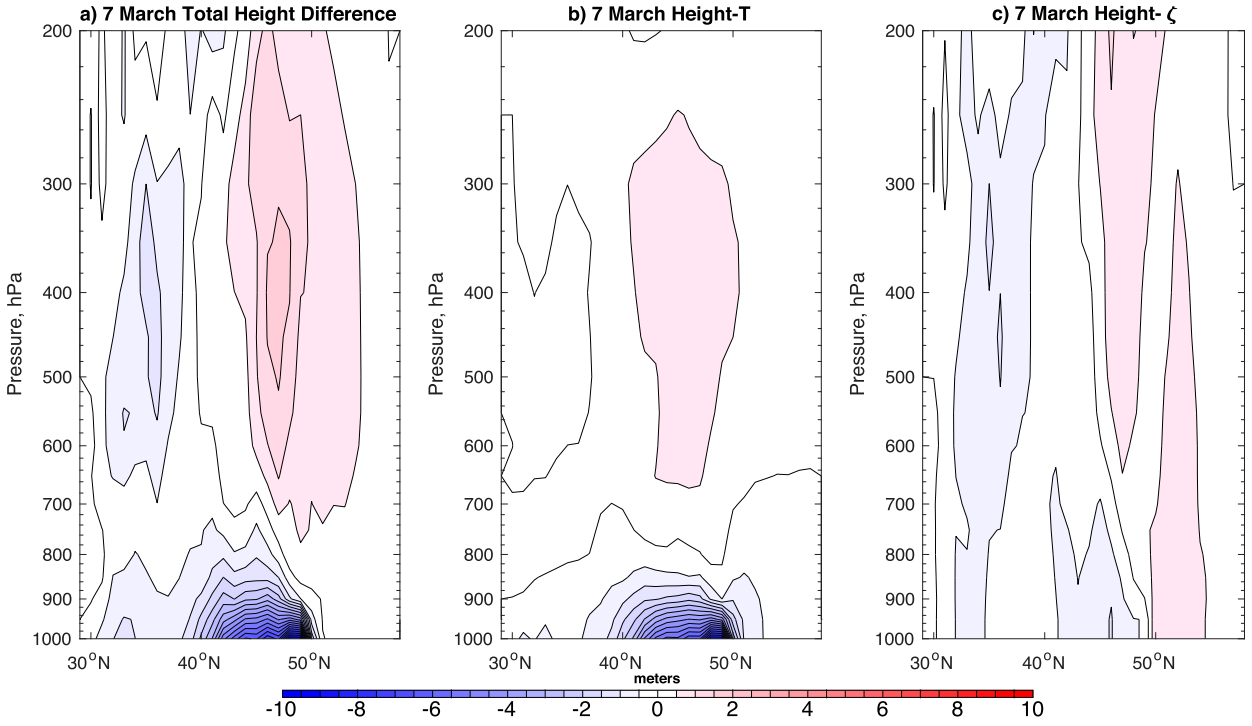

FIG. 6. Cross sections of the (a) total height change, (b) height change due to the z_T'' term, and (c) height change due to the z_ζ'' term. All fields were averaged from 268° to 270°E (location shown in Fig. 4b) from 0000 to 1800 UTC 7 Mar 2005.

observed early in the cyclone life cycle, an effect that deepens the developing cyclone. As the cyclone matures, however, the relative vorticity field produces an anticyclonic anomaly that extends to the surface and weakens the surface cyclone in its northwest quadrant (Fig. 3d). Thus while the direct response to the warm surface anomaly produced by removing snow acts according to our initial hypothesis, the response in the mid- and upper troposphere induced by the vorticity response to snow removal also influences the development of the surface cyclone.

b. *January 1996 case*

The January 1996 cyclone developed predominantly south of the snow line, in contrast to the March case that originated north of the snow line and propagated southeastward across it. The January case also developed in the wake of a predecessor cyclone, which was not the case for the March event. On 25 January, the cyclone was a small depression located in the central United States just south of the snow boundary and in a broad region of baroclinicity (Fig. 9a). The system propagated eastward over the next two days, its height minimum crossing to just north of the snow boundary on 27 January (Figs. 9b,c). At this time the cyclone also displayed a typical thermal structure including a warm sector, warm and cold fronts. One day later, the cyclone continued to deepen and also expanded notably in its horizontal extent, with its center located over the snow boundary in eastern Maine (Fig. 9d).

As in the previous case, negative 1000-hPa height anomalies result from the removal of snow, located over and south of the region where the snow was removed in the 90th-percentile simulation (Fig. 10). On 25 January, positive height anomalies were located north of the modified snow boundary over eastern Canada, over the northern portion of the predecessor cyclone (Fig. 10a). From 25 to 26 January negative height anomalies developed to the east of the developing cyclone in the central United States, with weakly negative anomalies located over the cyclone center (Figs. 10a,b). By 26 January, the positive anomalies observed over eastern Canada a day earlier had either weakened or propagated out of the model domain, along with the predecessor cyclone. On 27 January a strong couplet of negative and positive anomalies developed, straddling the amplifying cyclone located over Michigan, whose center was now located directly over the region of snow removal (Fig. 10c). By 28 January, the positive height anomalies west of the cyclone center on 27 January had expanded and appeared to have been advected southeastward by the cyclonic circulation of the system on its western edge (Fig. 10d). A region of negative height anomalies is observed north of the cyclone center, having weakened substantially compared to one day prior. The prevalence of negative height anomalies early in the cyclone life cycle, which transitions to a mix of positive and negative anomalies when the cyclone matures, is a common element between the two cases, while the exact position of the anomalies with respect to the cyclone center differs.

On 25 January, surface warm anomalies were roughly collocated with the negative height anomalies where snow was removed, as in the March case (Fig. 11a). Thereafter, however, a direct correspondence between the anomalous temperature and

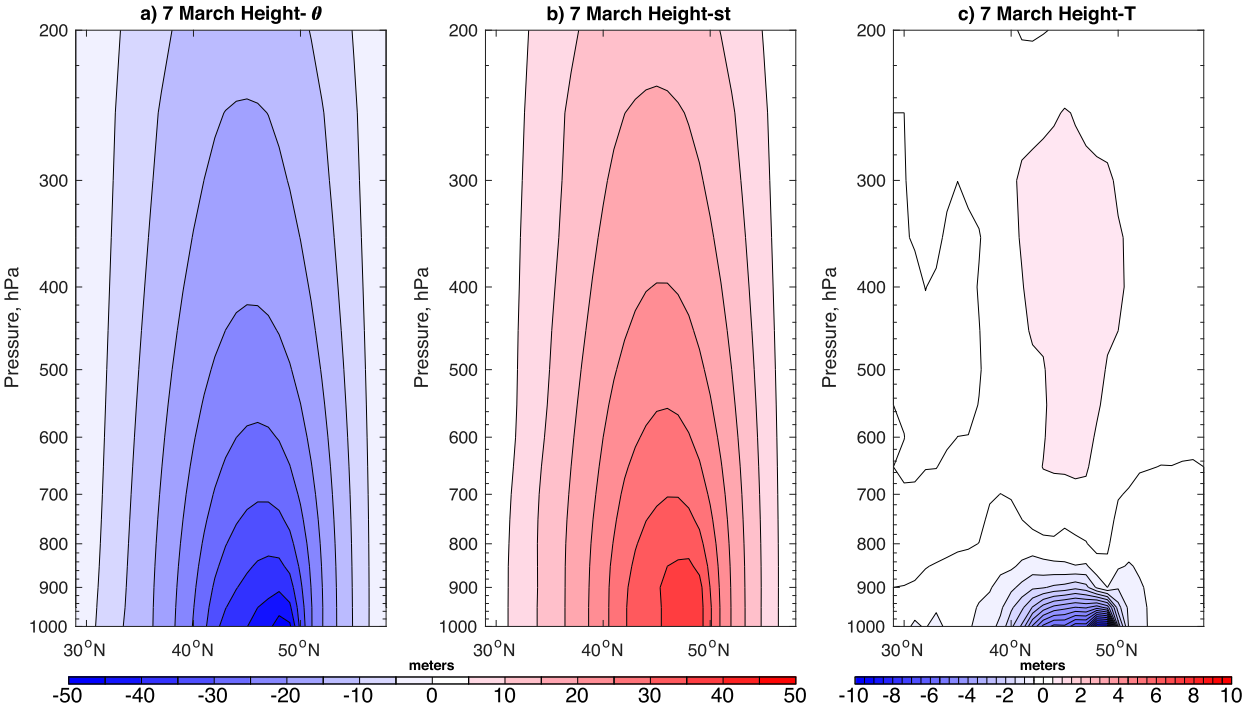

FIG. 7. Decomposition of the z''_T field into contributions from (a) z''_θ and (b) z''_{st} on 7 Mar 2005 along with (c) the net response z''_T. Note the change in the color scale relative to Fig. 6 and that (c) is the same field as in Fig. 6b.

height fields is not apparent, with, for instance, very strong warm anomalies located northwest of the cyclone on 26 January, where only weakly negative or neutral height anomalies were observed (cf. Fig. 11b, Fig. 10b). Warm anomalies remained within the region of snow removal over the Great Plains and upper Midwest through 28 January while the height anomalies underwent a substantially different evolution as the cyclone amplified and propagated eastward. This behavior is suggestive

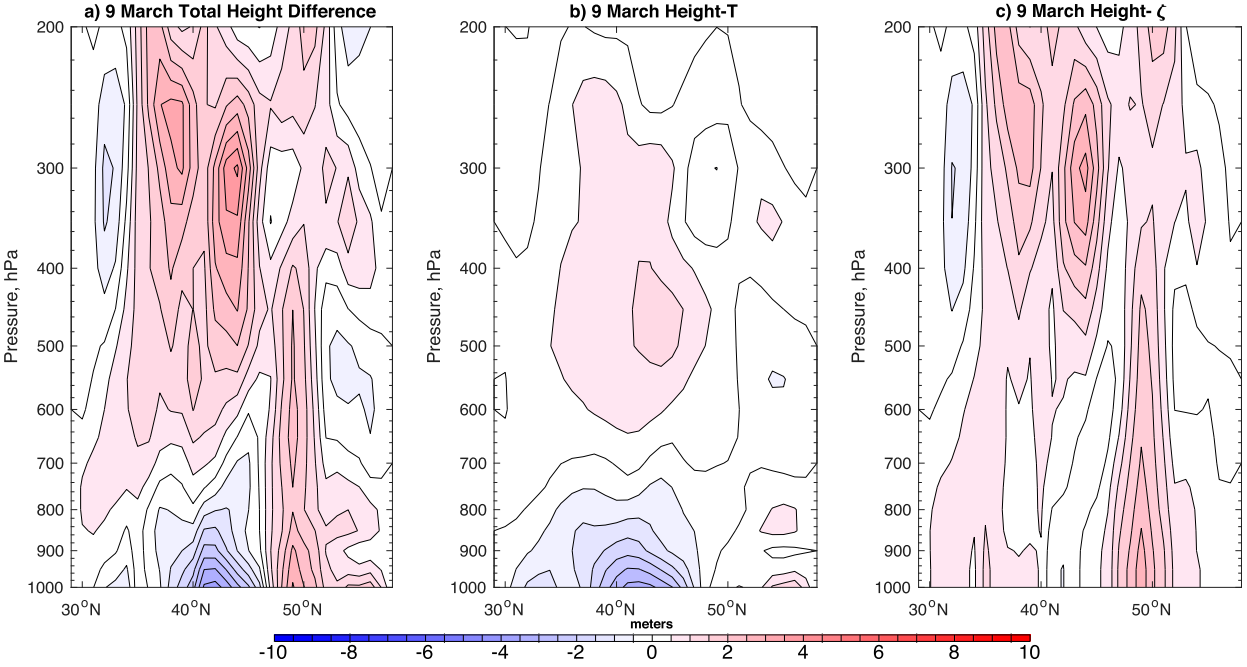

FIG. 8. As in Fig. 6, but averaged from 0000 to 1800 UTC 9 Mar 2005 and over longitudes 290°–292°E.

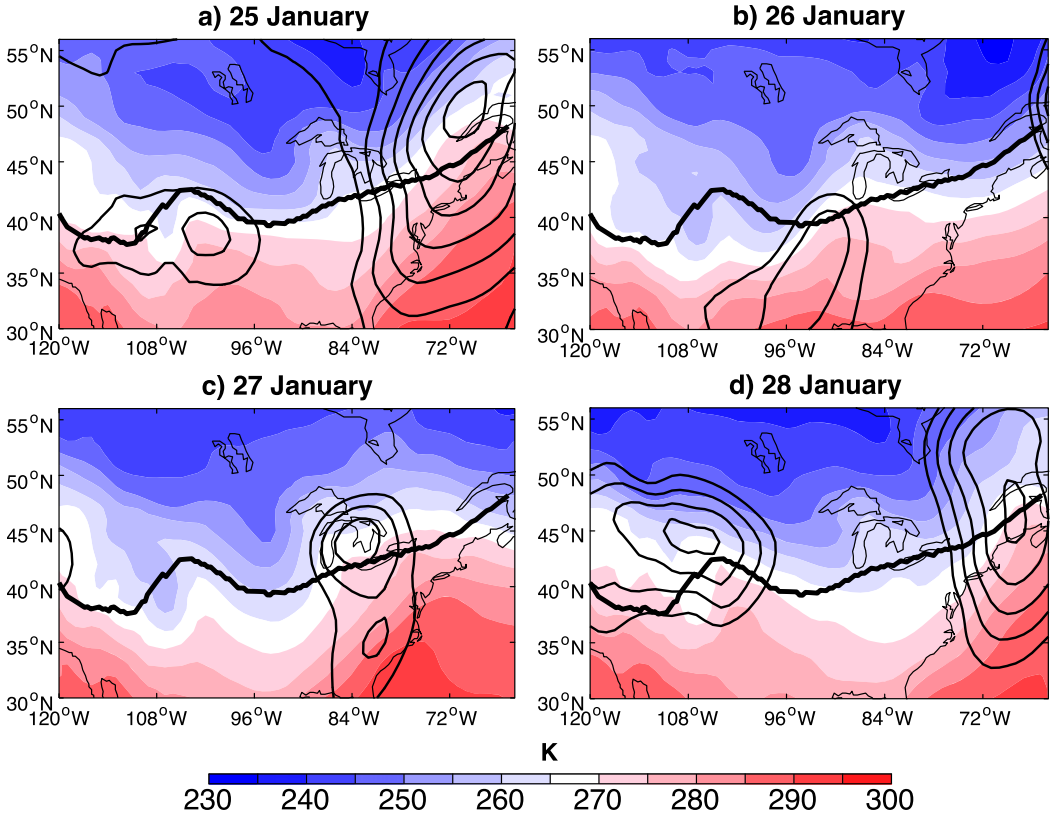

FIG. 9. The daily mean 1000-hPa temperature (color shading) and the 1000-hPa z' field (anomalies calculated with respect to the 0000 UTC 22 Jan–1800 UTC 28 Jan 1996 average; thin black contours, contoured every 25 m starting at −25 m), negative values only, for (a) 25, (b) 26, (c) 27, and (d) 28 Jan 1996. Fields are shown for the control simulation. The thick black line marks the location of the snow line in the control simulation.

of a stronger influence of the stability and relative vorticity contributions to the height field in this case, which obscured the correspondence between surface temperature anomalies and height anomalies observed more clearly in the March 2005 case. We note that there is no a priori reason to expect a direct correspondence between the height and surface temperature fields, but that the presence of such a relationship was suspected to be characteristic of the impact of snow removal on the circulation as suggested by Fig. 1.

Cross sections of height and temperature anomalies on 25 January show that the negative height anomalies and warm anomalies were greatest near the surface and gradually weakened with altitude, though not as rapidly as observed on 7 March in the previous case (cf. Fig. 12a,c, Figs. 5a,c). The height anomalies changed sign to positive near 600 hPa, peaking in strength at 300 hPa. Three days later on 28 January, the height response over the cyclone center (located at 45°N) reversed, with positive anomalies observed south of 50°N in the lower troposphere (Fig. 12b). The temperature anomaly pattern had also evolved into a broad, weak cold anomaly located near 40°–45°N at the surface, tilting northward with altitude to about 350 hPa (Fig. 12d). Only a small remnant of the previously strong surface warm anomaly remained, centered just north of 45°N. QGPV inversion will investigate which terms contributed to this dramatic reversal of the temperature and height fields.

Cross sections of the z''_T and z''_ζ contributions to the z'' field indicate that the former accounted for most of the negative height anomaly in the lower-troposphere and positive height anomalies in the mid- to upper troposphere, as observed in the March case (Figs. 13a,b). The relative vorticity contribution to the height field reinforced that induced by the temperature term, particularly at upper levels (Fig. 13c). The deeper vertical extent of the warm anomaly in this case compared to the March case (Fig. 12c) coincides with a deeper vertical extent of the negative height anomalies from the surface into the troposphere. Three days later on 28 January, the z''_T response reversed from its pattern on 25 January, and is associated with positive height anomalies in the lower troposphere and negative height anomalies above 600 hPa (Figs. 14a,b). The vorticity contribution to the height field had also changed and, by this time, accounted for the majority of the negative height anomalies observed throughout the troposphere north of 45°N and positive height anomalies at lower latitudes (Fig. 14c). In the net, the two components of the height field enhance one another near 40°N to produce the positive anomalies observed at 1000 hPa. The increase in the magnitude of the vorticity-induced anomalies later in the cyclone life cycle is similar to

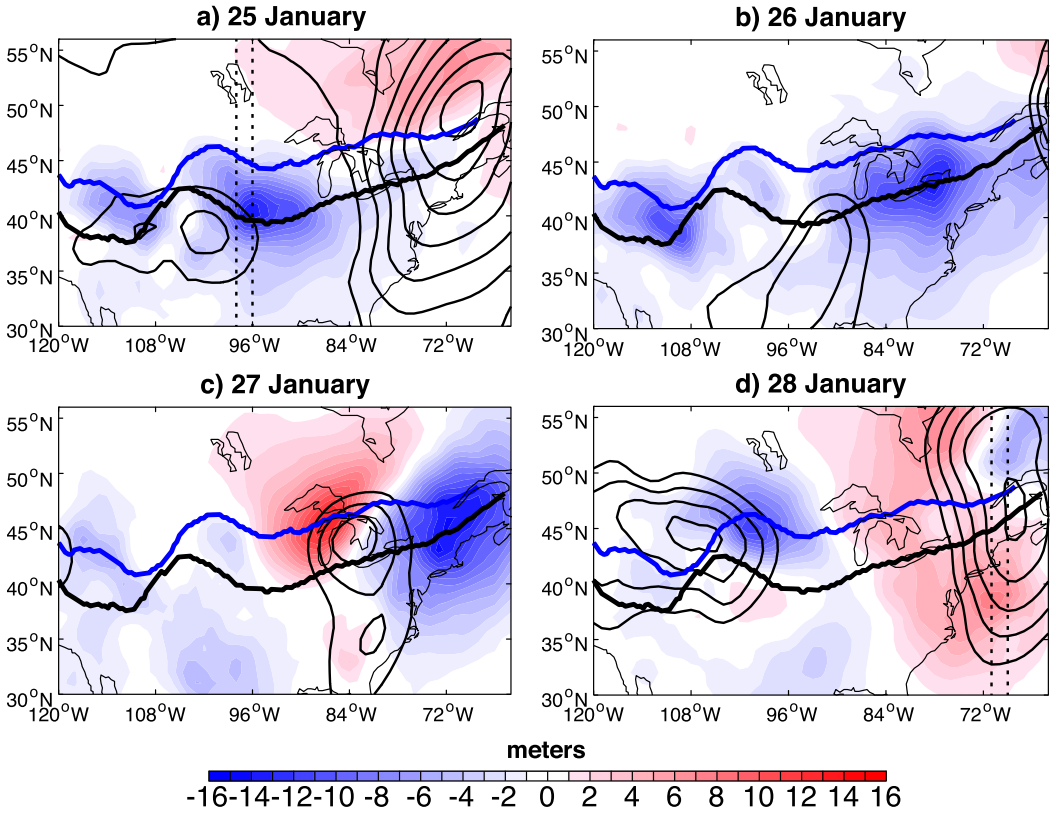

FIG. 10. The daily mean 1000-hPa z'' field (anomalies calculated as the difference: 90th-percentile simulation − control simulation; color shading) at (a) 25, (b) 26, (c) 27, and (d) 28 Jan 1996. The thin black contours show the 1000-hPa z' field, contoured every 25 m starting at −25 m, negative values only. The thick black line marks the location of the snow line in the control simulation, and the thick blue line shows the snow line in the 90th-percentile snow-removal simulation. The dashed lines in (a) and (d) mark the location of cross sections presented in Fig. 12, below.

that observed in the March case, although there is little similarity in the structure of the vorticity-induced height response between cases.

The complete sign reversal of the z''_T anomalies over the course of the life cycle, observed only in the January case, is another notable difference between the cases (Figs. 12a,b). This change could occur if the surface temperature anomaly changed sign from warm to cold, or if the stability term dominates over the direct temperature effect through changes in the vertical structure of the temperature field. While cold anomalies were observed in much of the lower troposphere, anomalies at 1000 hPa were weak but positive at 45°N (Fig. 12d). Decomposing the z''_T term on 28 January reveals that the 1000-hPa temperature anomaly induced a negative/cyclonic z''_θ anomaly, which was negated by a stronger, positive height anomaly produced by the stability term z''_{st} from 1000 to 700 hPa (Fig. 15). The negative anomalies produced by the surface temperature component are most likely driven by the nonlocal effect of the broad warm anomalies observed to the west of the location of the cross section at 1000 hPa (Fig. 11d). However, the stability term captures the vertical structure of the cold anomalies observed more directly over the cyclone center (Fig. 12d), producing height rises where the temperature anomalies decreased with altitude (Fig. 15b). The stability contribution is essentially highlighting how a strong surface warm anomaly, or midtropospheric cold anomaly, increases the environmental lapse rate and reduces the stability of the lower troposphere, creating a negative QGPV anomaly and a positive height anomaly. How the removal of snow led to a cold anomaly over the cyclone during its mature phase is not immediately clear, and suggests that snow removal can lead to a variety of indirect and potentially opposing effects, likely related to differences in the advection of temperature and vorticity between simulations.

4. Discussion and conclusions

We have investigated the short-term atmospheric response to a northward-shifted snow boundary during boreal winter for two cases selected for their differences regarding position relative to the snow line, time of year and origin. We found that the opposing effects of a surface warm anomaly, which simultaneously produces a cyclonic QGPV anomaly and a negative static stability anomaly, heavily influenced the height response

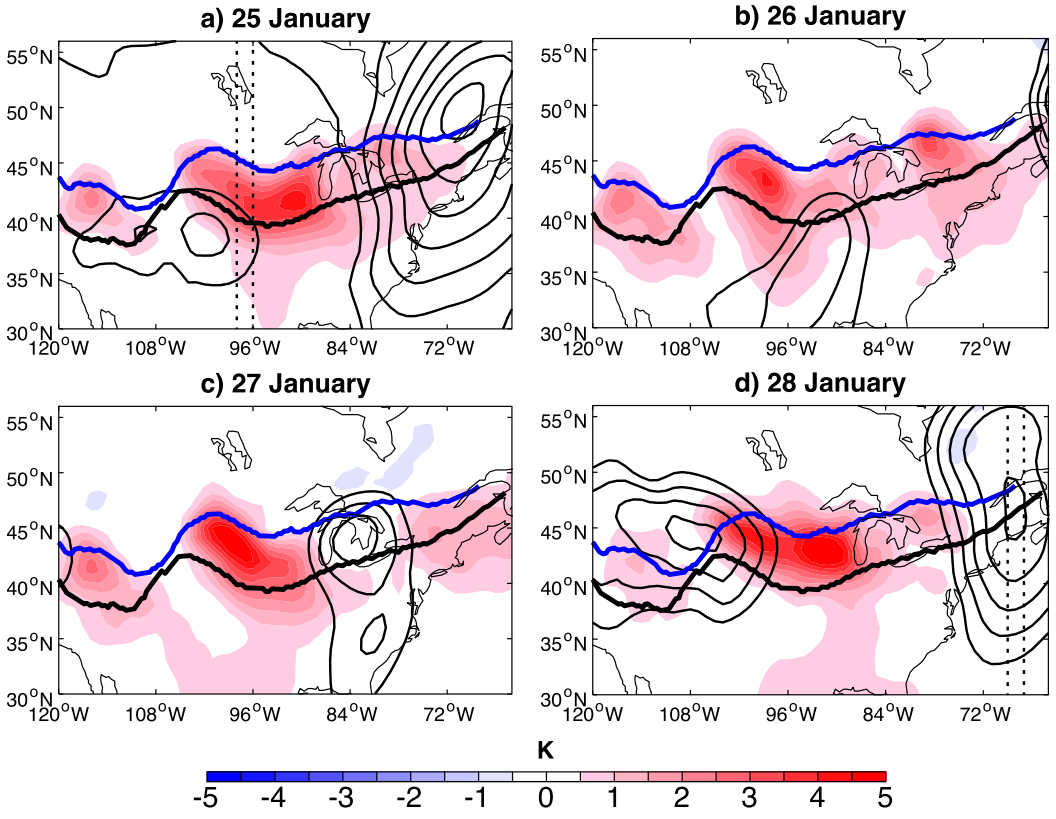

FIG. 11. As in Fig. 10, but with the color shading showing the 1000-hPa t'' anomalies.

near the surface. Our results are consistent with those of Elguindi et al. (2005), who found that increasing snow cover over the Great Plains weakened weather systems and enhanced lower-tropospheric stability. Here, we posed the opposite problem and found an opposite result, with stronger surface cyclone minima and reduced static stability.

In both cases investigated, the overall impact of snow removal early in the cyclone life cycle involved production of negative height anomalies that deepened the surface feature, while at upper levels positive height anomalies developed above the surface warm anomalies. The structure of the temperature and height fields in the nascent stage of the cyclone life cycle in both cases is similar to the structure of ''thermal lows'' that often develop over arid regions in the subtropics (Ramage 1971; Rowson and Colucci 1992). Thermal lows develop from strong surface heating and have a nonfrontal cyclonic circulation, most commonly confined to below 700 hPa, with the circulation weakening and often becoming anticyclonic higher in the troposphere (Petty 2008), as observed in these two cases.

As the relative vorticity contribution to heights strengthened later in the cyclone life cycle, the height response in both cases involved development of positive height anomalies west of the surface cyclone center (cf. Fig. 3 and Fig. 10). The advection of height anomalies by the circulation likely assisted in generating stronger horizontal gradients, subsequently increasing the magnitude of the anomalies themselves. At upper levels, the height response near the cyclone center differed. Whereas the March 2005 case was characterized by positive height anomalies, the January 1996 case featured a dipole of negative anomalies north of the cyclone center and positive anomalies to its south. It is likely that the upper-tropospheric differences between the two cases are related to the change in the temperature structure near the cyclone center. The cold temperature anomalies observed on 28 January, associated with reduced thickness, would be consistent with lower heights above the temperature anomaly, producing a cyclonic anomaly at upper levels. In the March case, the temperature anomaly consistently contributed a cyclonic anomaly, while the vorticity term contributed an anticyclonic anomaly. Despite these differences, in both cases the relative vorticity response to snow removal strengthened later in the cyclone life cycle, ultimately dominating the height response.

Our results are roughly consistent with what Ellis and Leathers (1998) found as well, namely that the inclusion of snow cools the surface and removal warms the surface. Their study used a one-dimensional snowpack model to investigate the dynamics within cold air masses, which assumed temperature advection by the large-scale circulation was minimal. Our study, in contrast, highlights the life cycle-dependent evolution of the temperature response engendered by removing snow. We find that the advection of the initial height response to snow removal by the cyclone itself generated vorticity, which subsequently produced its own height response. We therefore

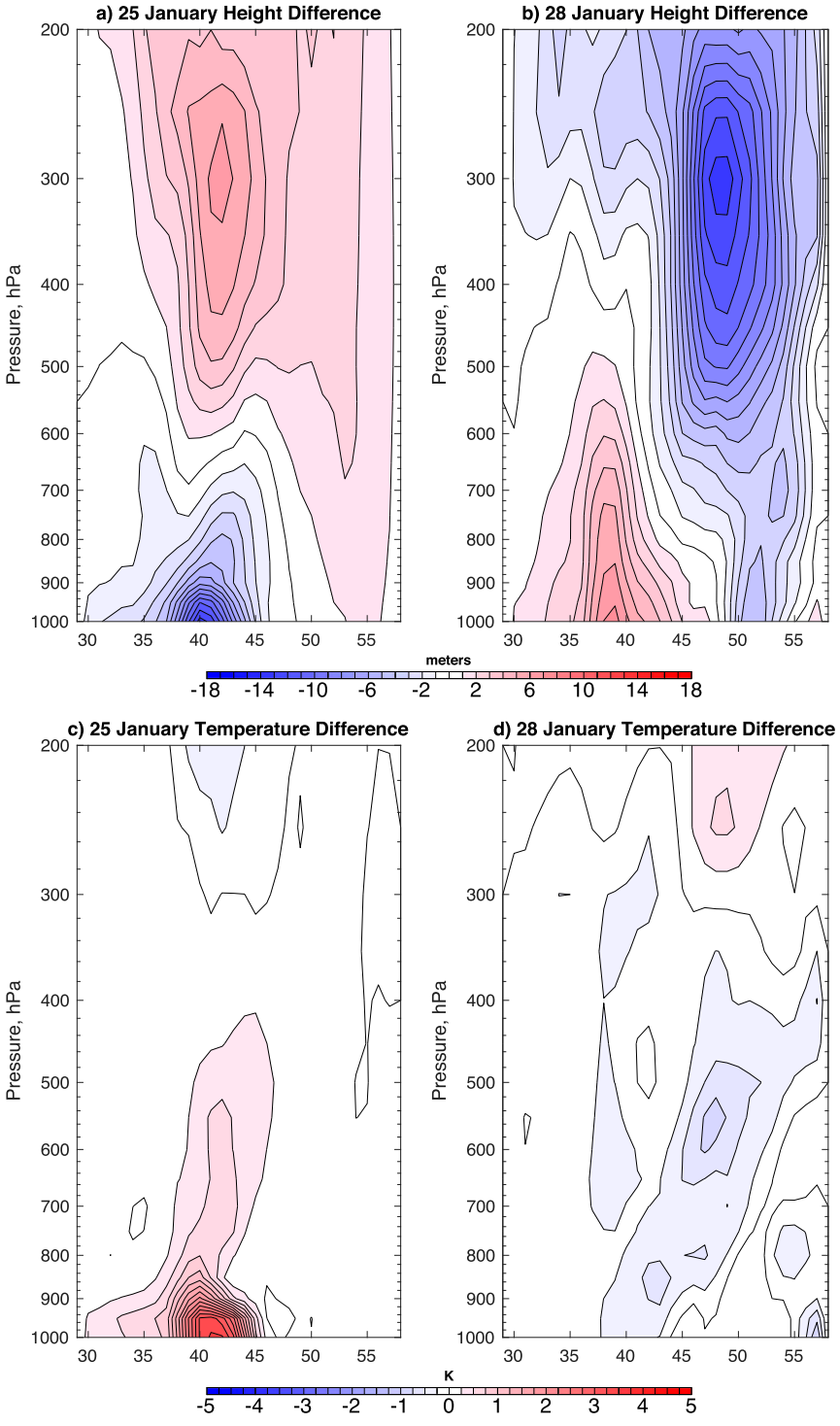

FIG. 12. Cross sections of (a),(b) geopotential height and (c),(d) temperature averaged over the locations indicated in Fig. 11 on (left) 25 and (right) 28 Jan 1996.

note that, when analyzing changes in the circulation that arise due to changing snow cover, advection must be considered along with in situ interactions between the surface and overlying atmosphere.

Through this analysis the initial hypothesis was confirmed; namely, that a surface warm anomaly would be produced by removing snow, and would lead to development of a cyclonic QGPV anomaly and negative height anomaly. Somewhat

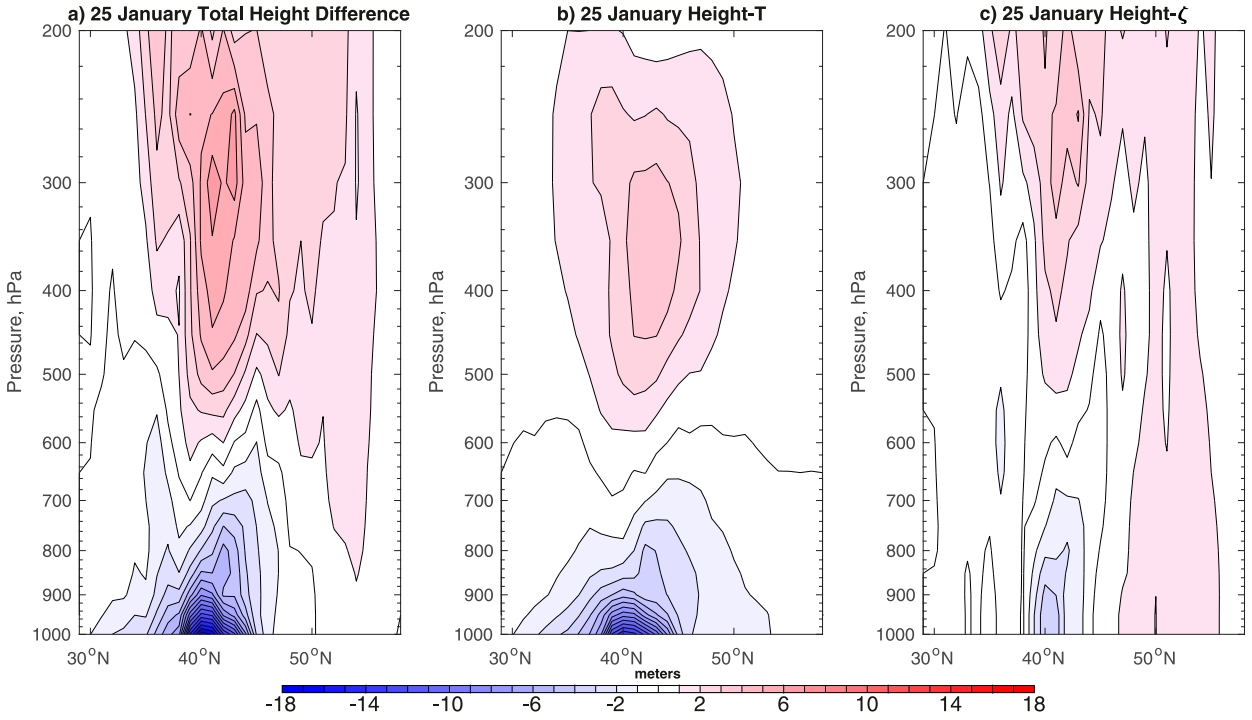

FIG. 13. Cross sections of the (a) total height change, (b) height change due to the z_T'' term, and (c) height change due to the z_ζ'' term. All fields were averaged from 262° to 264°E (location shown in Fig. 11a) from 0000 to 1800 UTC 25 Jan 1996.

unexpectedly, the analysis also revealed that this effect is most notable early in the cyclone life cycle and can be negated or enhanced by the response in the vorticity field. The interplay between the temperature and wind responses when the lower boundary changes is thus further elucidated, suggesting that the overall response of developing cyclones to snow removal may be a small residual of two substantial but opposing forcings. The surface warm anomaly, being a

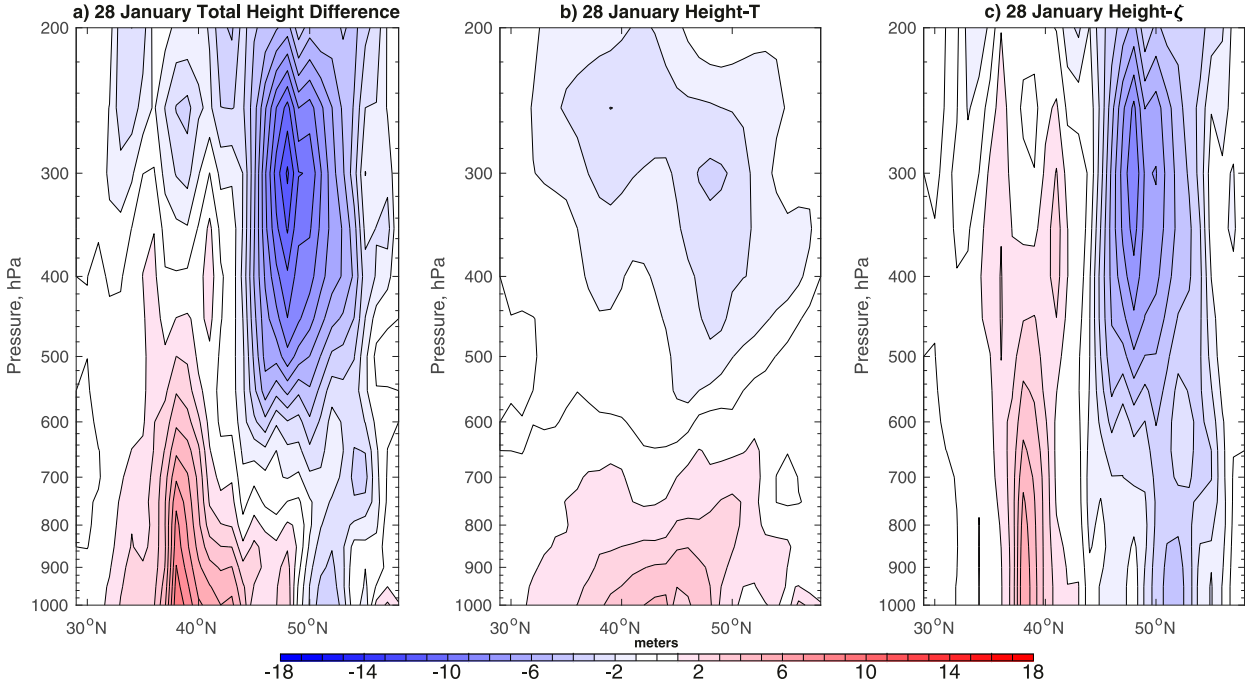

FIG. 14. As in Fig. 13 but averaged from 289° to 291°E from 0000 to 1800 UTC 28 Jan 1996.

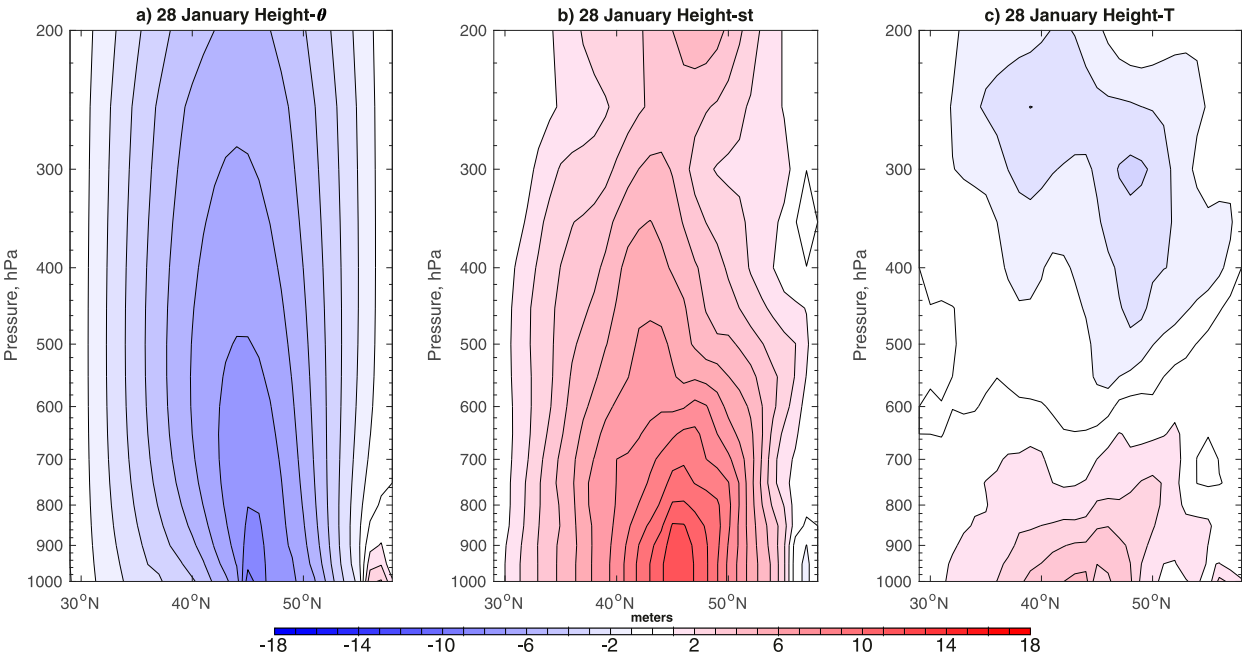

FIG. 15. Decomposition of the z_T'' field into contributions from (a) z_θ'' and (b) $z_{\rm st}''$ on 28 Jan 1996 along with (c) the net response z_T''.

surrogate positive PV anomaly, serves to induce negative height anomalies. As in the March 2005 case, the surface warming can simultaneously lead to increased heights aloft via hypsometry. These local height increases induce an anticyclonic vorticity anomaly aloft whose influence can extend back down to the surface and manifest itself as opposing positive height anomalies. Alternatively, a cold anomaly developed in the lower troposphere in the January 1996 case near the cyclone center, suggesting that mixing and advection of air masses can oppose the surface warm anomaly initially produced by removing snow.

In sum, the effects of removing snow on the cyclone life cycle are observed and quantifiable but are generally transient and, even at their strongest, limited in magnitude and effect. Large, permanent changes to cyclone intensity and trajectory due to changes in the snow boundary do not seem likely when the snow removal leads cyclogenesis on daily time scales. We emphasize that the long-term, nonlocal impacts of a receding snow line were not the target of this analysis and could still have a large effect on the circulation, but the immediate, direct effects of snow removal appear to be relatively minimal through the mitigating responses of various components of the circulation. It is important to note that just two cases have been analyzed in this study, with the goal of exploring the possible ways in which snow removal *could* affect the cyclone life cycle. However, statistical analysis of a larger number of cases from the same model case studies reveals a relatively similar effect across all cases (Clare 2018). Additionally, other features of storm evolution, including precipitation type, mesoscale "snow breeze" circulations, or cloud microphysics were not investigated, and could be influenced by the snow cover change. Future work could apply the same methods employed here to a larger sample of the simulations to better understand the average response of midlatitude cyclones to a northward-shifted snow boundary.

We note that the nature of the conducted experiments is highly idealized, and does not consider any future changes to the background state, such as enhanced moisture and baroclinicity, induced by climate shifts unrelated to snow removal. Simulations in the future could combine snow-removal-induced changes with modifications to the background state, such as increased warming and moisture, to determine how the snow removal response interacts with a realistically modified background. Changes in stability that are unrelated to snow removal, for instance, could either reinforce or negate the changes that arise due to snow. Last, the response of surface anticyclogenesis, which is more susceptible to radiative effects, to snow removal is a subject of ongoing work.

Acknowledgments. The authors acknowledge support for this project by the University of Wisconsin Office of the Vice Chancellor for Research and Graduate Education Fall Research Competition and the National Science Foundation Climate and Large-Scale Dynamics Program Award (NSF AGS-1640452**).** This research was supported by the NOAA Climate and Global Change Postdoctoral Fellowship Program, administered by UCAR's Cooperative Programs for the Advancement of Earth System Science (CPAESS) under Award NA18NWS4620043B. We also acknowledge technical support from the UW Advanced Computing Initiative (ACI) Center for High Throughput Computing (CHTC). We also acknowledge Dr. Michael Notaro for assistance with model simulations.

Data availability statement. All model outputs were submitted to the Environmental Data Initiative (EDI) repository and are available at Clare et al. (2020).

REFERENCES

Bretherton, F. B., 1966: Critical layer instability in baroclinic flows. *Quart. J. Roy. Meteor. Soc.*, **92**, 325–334, https://doi.org/10.1002/qj.49709239302.

Brown, R. D., 2000: Northern Hemisphere snow cover variability and change, 1915–97. *J. Climate*, **13**, 2339–2355, https://doi.org/10.1175/1520-0442(2000)013<2339:NHSCVA>2.0.CO;2.

Brutel-Vuilmet, C., M. Menegoz, and G. Krinner, 2013: An analysis of present and future seasonal Northern Hemisphere land snow cover simulated by CMIP5 coupled climate models. *Cryosphere*, **7**, 67–80, https://doi.org/10.5194/tc-7-67-2013.

Clare, R. M., 2018: Modelled response of extratropical cyclone cases in the Great Plains to projected late twenty-first century snow cover extents. M.S. thesis, Department of Atmospheric and Oceanic Sciences, University of Wisconsin–Madison, 71 pp., http://digital.library.wisc.edu/1793/80597.

——, A. R. Desai, M. Notaro, J. E. Martin, and S. J. Vavrus, 2020: Projected Snow Cover Reductions and Midlatitude Cyclone Responses in the North American Great Plains, 1986–2005, version 2. Environmental Data Initiative, https://doi.org/10.6073/pasta/2f9cdf9caa9ee16bc4cbf4935b881da6.

Elguindi, B. H., B. Hanson, and D. Leathers, 2005: The effects of snow cover on midlatitude cyclones in the Great Plains. *J. Hydrometeor.*, **6**, 263–279, https://doi.org/10.1175/JHM415.1.

Ellis, A. W., and D. J. Leathers, 1998: A quantitative approach to evaluating the effects of snow cover on cold air mass temperatures across the U.S. Great Plains. *Wea. Forecasting*, **13**, 688–701, https://doi.org/10.1175/1520-0434(1998)013<0688:AQATET>2.0.CO;2.

——, and ——, 1999: Analysis of cold airmass temperature modification across the US Great Plains as a consequence of snow depth and albedo. *J. Appl. Meteor.*, **38**, 696–711, https://doi.org/10.1175/1520-0450(1999)038<0696:AOCATM>2.0.CO;2.

Gan, T. Y., R. G. Barry, M. Gizaw, A. Gobena, and R. Balaji, 2013: Changes in North American snowpacks for 1979-2007 detected from the snow water equivalent data of SMMR and SSM/I passive microwave and related climatic factors. *J. Geophys. Res.*, **118**, 7682–7697, https://doi.org/10.1002/jgrd.50507.

Holopainen, E., and J. Kaurola, 1991: Decomposing the atmospheric flow using potential vorticity framework. *J. Atmos. Sci.*, **48**, 2614–2625, https://doi.org/10.1175/1520-0469(1991)048<2614:DTAFUP>2.0.CO;2.

Klingaman, N. P., B. Hanson, and D. J. Leathers, 2008: A teleconnection between forced Great Plains snow cover and European winter climate. *J. Climate*, **21**, 2466–2483, https://doi.org/10.1175/2007JCLI1672.1.

Lavaysse, C., C. Flamant, S. Janicot, D. J. Parker, J.-P. Lafore, B. Sultan, and J. Pelon, 2009: Seasonal evolution of the west African heat low: A climatological perspective. *Climate Dyn.*, **33**, 313–330, https://doi.org/10.1007/s00382-009-0553-4.

Lemke, P., and Coauthors, 2007: Observations: Changes in snow, ice, and frozen ground. *Climate Change 2007: The Physical Science Basis*, S. Solomon et al., Eds., Cambridge University Press, 339–383.

Manabe, S., and R. T. Wetherald, 1980: On the distribution of climate change resulting from an increase in CO_2 content of the atmosphere. *J. Atmos. Sci.*, **37**, 99–118, https://doi.org/10.1175/1520-0469(1980)037<0099:OTDOCC>2.0.CO;2.

Petty, G. W., 2008: *A First Course in Atmospheric Thermodynamics*. Sundog Publishing, 337 pp.

Ramage, C. S., 1971: *Monsoon Meteorology*. Academic Press, 296 pp.

Ross, B., and J. E. Walsh, 1986: Synoptic-scale influences of snow cover and sea ice. *Mon. Wea. Rev.*, **114**, 1795–1810, https://doi.org/10.1175/1520-0493(1986)114<1795:SSIOSC>2.0.CO;2.

Rowson, D. R., and S. J. Colucci, 1992: Synoptic climatology of thermal low-pressure systems over south-western North America. *Int. J. Climatol.*, **12**, 529–545, https://doi.org/10.1002/joc.3370120602.

Rydzik, M., and A. R. Desai, 2014: Relationship between snow extent and midlatitude disturbance centers. *J. Climate*, **27**, 2971–2982, https://doi.org/10.1175/JCLI-D-12-00841.1.

Skamarock, W. C., and Coauthors, 2019: A description of the Advanced Research WRF Model version 4. NCAR Tech. Note NCAR/TN-556+STR, 145 pp., https://doi.org/10.5065/1dfh-6p97.

Sobolowski, S., G. Gong, and M. Ting, 2010: Modeled climate state and dynamic response to anomalous North American snow cover. *J. Climate*, **23**, 785–799, https://doi.org/10.1175/2009JCLI3219.1.